

A. Ekedahl, K. Rantamäki, M. Goniche, J. Mailloux, V. Petrzilka, G. Granucci, B. Alper, G. Arnoux, Y. Baranov, V. Basiuk, P. Beaumont, G. Calabrò, V. Cocilovo, G. Corrigan, L. Delpéch, K. Erents, D. Frigione, N. Hawkes, J. Hobirk, F. Imbeaux, E. Joffrin, K. Kirov, T. Loarer, D. McDonald, M. F. F. Nave, I. Nunes, J. Ongena, V. Parail, F. Piccolo, E. Rachlew, C. Silva, A. Sirinelli, M. Stamp, K-D. Zastrow
and JET EFDA contributors

Effect of Gas Injection during LH Wave Coupling at ITER-Relevant Plasma-Wall Distances in JET

“This document is intended for publication in the open literature. It is made available on the understanding that it may not be further circulated and extracts or references may not be published prior to publication of the original when applicable, or without the consent of the Publications Officer, EFDA, Culham Science Centre, Abingdon, Oxon, OX14 3DB, UK.”

“Enquiries about Copyright and reproduction should be addressed to the Publications Officer, EFDA, Culham Science Centre, Abingdon, Oxon, OX14 3DB, UK.”

Effect of Gas Injection During LH Wave Coupling at ITER-Relevant Plasma-Wall Distances in JET

A. Ekedahl¹, K. Rantamäki², M. Goniche¹, J. Mailloux³, V. Petržilka⁴, G. Granucci⁵, B. Alper³,
G. Arnoux¹, Y. Baranov³, V. Basiuk¹, P. Beaumont³, G. Calabrò⁶, V. Cocilovo⁶, G. Corrigan³,
L. Delpech¹, K. Erents³, D. Frigione⁶, N. Hawkes³, J. Hobirk⁷, F. Imbeaux¹, E. Joffrin¹,
K. Kirov⁷, T. Loarer¹, D. McDonald³, M. F. F. Nave⁸, I. Nunes⁸, J. Ongena⁹, V. Parail³,
F. Piccolo³, E. Rachlew¹⁰, C. Silva⁸, A. Sirinelli³, M. Stamp³, K-D. Zastrow³
and JET EFDA contributors*

JET-EFDA, Culham Science Centre, OX14 3DB, Abingdon, UK

¹CEA, IRFM, F-13108 Saint-Paul-lez-Durance, France.

²Association Euratom-Tekes, VTT, PO Box 1000, FI-02044 VTT, Espoo, Finland.

³Association Euratom-UKAEA, Culham Science Centre, Abingdon, Oxon, OX14 3DB, UK.

⁴Association Euratom-IPP, CR, IPP AS CR, Za Slovankou 3, 182 21 Praha 8, Czech Republic.

⁵Association Euratom-ENEA sulla Fusione, IFP Milano, Italy.

⁶Association Euratom-ENEA sulla Fusione, C.R. Frascati, Roma, Italy.

⁷Association Euratom-MPI für Plasmaphysik D-85748 Garching, Germany.

⁸Association Euratom-IST, Centro de Fusão Nuclear, IST, 1049-001 Lisbon, Portugal.

⁹Association Euratom-Belgian State, ERM-KMS, B-1000 Brussels Belgium.

¹⁰Association Euratom-VR, Department of Physics, SCI, KTH, SE-10691 Stockholm, Sweden.

* See annex of M.L. Watkins et al, "Overview of JET Results",
(Proc. 21st IAEA Fusion Energy Conference, Chengdu, China (2006)).

ABSTRACT.

Good coupling of Lower Hybrid (LH) waves has been demonstrated in different H-mode scenarios in JET, at high triangularity ($\delta \sim 0.4$) and at large distance between the LCFS and the LH launcher (15cm). Local gas injection of D_2 in the region magnetically connected to the LH launcher is used for increasing the local density in the scrape-off layer (SOL). Reciprocating Langmuir probe measurements magnetically connected to the LH launcher indicate that the electron density profile flattens in the far SOL during gas injection and LH power application. Some degradation in normalised H-mode confinement, as given by the $H_{98}(y,2)$ -factor, could be observed at high gas injection rates in these scenarios, but this was rather due to total gas injection and not specifically to the local gas puffing used for LH coupling. Furthermore, experiments carried out in L-mode plasmas in order to evaluate the effect on the LH current drive efficiency, when using local gas injection to improve the coupling during large distance between the separatrix and the launcher, indicate a small degradation ($\Delta I_{LH}/I_{LH} \sim 15\%$). This effect is largely compensated by the improvement in coupling and thus increase in coupled power when using gas puffing.

1. INTRODUCTION

Lower hybrid (LH) waves are one of the most efficient methods for non-inductive current drive generation in a tokamak. LH waves have the property of damping efficiently at high parallel phase velocities, v_{\parallel} , relative to the electron thermal speed [1]. They are therefore well suited for driving current off-axis in the plasma where the electron temperature is lower. Localised current off-axis gives a method for current profile control, which is crucial for the so called advanced tokamak scenarios relying on the formation of an internal transport barrier (ITB) [2]. Lower Hybrid Current Drive (LHCD) is used routinely in the advanced tokamak scenarios in JET, both for tailoring the target q-profile in the plasma current ramp-up phase before the main heating, as well as during the main heating phase in order to maintain the desired q-profile for longer duration [3].

The coupling of the slow wave to the plasma is a crucial issue, in particular for the next step device, ITER. The presence of a cut-off density, n_{co} , below which the slow wave does not propagate, necessitates the ability to control the electron density in front of the LH launcher. The cut-off density corresponds to the density at which the launched wave frequency equals the local electron plasma frequency. This gives $n_{co} = 0.0124 \times f^2$, where f is the launched wave frequency. For the LHCD system in JET, which operates at $f = 3.7\text{GHz}$, n_{co} equals $1.7 \times 10^{17} \text{m}^{-3}$. In present day machines, the appropriate electron density for coupling conditions (typically $2-5 \times n_{co}$) can be obtained by moving the launcher or the plasma radially during the pulse. However, in ITER, the launcher will be imbedded in the first wall and the distance between the first wall and the Last Closed Flux Surface (LCFS) of the plasma will be as large as 15-20cm. In addition, the H-mode with its edge transport barrier causes a steep gradient in electron density, which makes the electron density at the first wall drop during the period between ELMs. Consequently, it is essential to demonstrate the feasibility of coupling LH waves on present day devices in conditions as close as possible to those of ITER,

and thus to find suitable methods for controlling the electron density.

In JET, local gas injection in the vicinity of the LH launcher has proven efficient for raising the electron density in front of the launcher, thereby improving the LH coupling. The idea of a local gas injection system originates from the results obtained in ASDEX [4] and such a system is now used routinely when coupling LH waves in H-mode plasmas in JET. Because of its size, JET is a unique device which enables coupling studies over large plasma-launcher distances, close to those expected in ITER. In recent campaigns, dedicated LH coupling experiments have been performed in ELMy H-mode plasmas with high triangularity, with q-profiles characteristic of the advanced tokamak scenario ($q_{95} \sim 5.5 - 7$) as well as the hybrid scenario ($q_{95} \sim 4$). In addition to the effect on the LH coupling, these experiments allowed to investigate the effect of gas puffing on the confinement properties of the plasma, in order to assess possible deleterious effects when using gas puffing for LH coupling control. The question of a possible degradation in LH current drive efficiency when using near gas injection was addressed in a recent experiment, carried out in L - mode plasmas.

2. THE LOWER HYBRID LAUNCHER IN JET

The LH launcher at JET [5, 6] operates at $f = 3.7\text{GHz}$ and is composed of 48 multijunctions, made of copper coated stainless steel, and mounted in 6 rows and 8 columns. The 48 multijunctions are fed by 24 klystrons, each capable of delivering 500kW for 20s. At the front face of each multijunction there are two rows with four narrow waveguides, with dimensions $9\text{mm} \times 72\text{mm}$. The total size of the launcher is therefore 0.9m height and 0.4m width, consisting of twelve rows with 32 active waveguides. The n_{\parallel} spectrum radiated from the launcher is usually centred at $n_{\parallel} = 1.84$. n_{\parallel} can be varied between 1.4 and 2.3 by varying the phase difference between klystrons feeding adjacent multijunctions, from -90° to $+90^{\circ}$. $n_{\parallel} = 1.84$ and 2.3 was used in the experiments presented in this paper.

The launcher mouth is surrounded by a side protection frame to protect it from plasma radiation. In addition, poloidal limiters are positioned around the outer wall of the torus, protruding in front of the LH launcher and the Ion Cyclotron Resonance Heating (ICRH) antennas. In order to allow for good coupling in different plasma conditions, the launcher can be moved radially during the pulse. Typically the launcher is positioned between 5mm and 25mm behind the poloidal limiters.

In addition to the launcher position control, good coupling is achieved using a specially designed gas pipe, denoted GIM6 (Gas Introduction Module 6), which provides local gas flow near the launcher. The pipe is located on the outer wall about 1.2m from the launcher (figure 1). The first experiments with local gas injection for LH coupling were carried out in L-mode plasmas in 1996-1997 and later in H-mode plasmas from 2001 onwards, where both CD_4 injection [7] and D_2 injection [8] were used. D_2 injection proved to be more efficient than CD_4 to increase the electron density in the scrape-off layer (SOL), probably because D_2 gives higher recycling [8]. The previous LH coupling experiments in H-mode plasmas were limited mainly to low triangularity plasmas and to a distance between the Last Closed Flux Surface (LCFS) and the LH launcher of 11cm. In the work presented in this paper, good LH coupling was demonstrated in H-mode plasmas at high

triangularity, with maximum values of upper and lower triangularity of $\delta_{\text{up}} = 0.45$ and $\delta_{\text{low}} = 0.52$, and at LCFS-launcher distances up to 15cm.

3. LH COUPLING IN H-MODE PLASMAS

3.1. ADVANCED TOKAMAK SCENARIO

In recent campaigns dedicated experiments were performed to demonstrate LH coupling at large plasma-launcher distances [9]. These experiments were performed in an ELMy H-mode scenario that was used for the development of Advanced Tokamak scenarios with Internal Transport Barrier (ITB). However, since the experiments were performed early in the campaign during the development of the scenario, no ITBs were yet obtained. The magnetic field was between $B_T = 3.0\text{T}$ and 3.1T and the plasma current was $I_p = 1.5\text{-}1.9\text{MA}$, resulting in $q_{95} \sim 5.5 - 7$. In order to obtain an H-mode, Neutral Beam Injection (NBI) power ranging from 14MW to 18MW was used. In addition, up to 3MW ICRH power was used in some pulses. The LHCD power varied from 0 to 3.1MW and the launcher position was 2cm behind the poloidal limiter, while the LCFS was pushed 13cm away from the poloidal limiters. This distance is also denoted Radial Outer Gap (ROG). Figures 2 and 3 show two similar discharges in terms of injected powers, plasma position and GIM6 flow. The only difference between the two discharges is the fact that pulse #67882 has strong additional gas puffing from the gas injection points near the divertor region. One can note that the $H\alpha$ signal is therefore higher in #67882. As a consequence, the LH coupling during the period 4-6s is better in #67882 (figure 2) than in #67884 (figure 3). In #67884, the ragged LHCD power waveform during the period 4-6s is due to frequent interrupts caused by a launcher protection system that reduces the klystron output power when the reflected power is too high. When gas injection from GIM6 (4×10^{21} el/s) is switched on, the electron density increases, the reflection coefficient decreases and the coupled LHCD power is maintained above 2MW. In addition, one can note that the ICRH power suffers less trips when GIM6 is switched on, showing that coupling of ICRH can also be improved by local gas puffing [10].

With gas injection from the divertor at a rate 20×10^{21} el/s, and without gas injection from GIM6, good LH coupling was obtained on the upper and middle part of the launcher, as is demonstrated in #67882, 4-6s. Consequently, 2.4MW was stationary coupled to the plasma for 5s over a LCFS-launcher distance of 15cm and a reflection coefficient as low as $R_c = 6\%$. However, the lower part of the launcher has a reflection coefficient of about $R_{\text{clow}} = 10\%$. This poor coupling could be linked to the fact that the lowest row is furthest away from the plasma. The distance between the LCFS and the poloidal limiter is 14cm for the lowest row and 12-13cm for the other rows. When gas is injected from GIM6, the coupling on the bottom row is improved and the reflection coefficient of that row is restored to $R_{\text{clow}} = 2\%$.

A reciprocating Langmuir Probe (RCP) [11] was used to measure the far SOL plasmas in between ELMs. This probe is located at the top of the torus. The plasma scenario was chosen in such a way that the probe was magnetically connected to the LH launcher and the gas pipe GIM6. The measurements

were performed at $t = 5\text{s}$ and $t = 7\text{s}$ in #67884. Each reciprocation take approximately 200ms. In order to avoid disturbing the probe signal due to ICRH, the ICRH power was decreased during the reciprocations. The radial profile of the ion saturation current, J_{sat} , measured at two different times in #67884 are shown in figure 4. The ion saturation current can be considered proportional to the electron density. With gas puffing from GIM6 together with 2MW of coupled LHCD power, the J_{sat} -profile flattens in the far SOL, i.e. typically between 8cm and 15cm from the LCFS (squares). At 15cm, which is the radial location of the LH launcher, the ion saturation current is more than twice as large as compared to the case without gas injection (circles). The location of the poloidal limiter is indicated by the dashed line at 13cm. However, closer to the separatrix basically no difference is seen in J_{sat} .

3.2. ADVANCED TOKAMAK SCENARIO

For the first time in JET, LHCD power has been coupled during the H-mode phase of low toroidal magnetic field plasmas ($B_T = 1.7\text{T}$, $I_p = 1.4\text{MA}$, $q_{95} = 4$). This configuration was used for studying the Hybrid scenario in JET [12] and its comparison to the standard H-mode scenario. The aim of the experiment was to demonstrate the LH coupling capability in high triangularity plasmas with large LCFS-launcher distance and during ELMs, in a similar way as in the advanced tokamak configuration described above. Also in this scenario at low toroidal magnetic field, good coupling of the LH wave was obtained at a distance between the LCFS and the launcher of 14cm, using D2 injection from GIM6. This is shown in figure 5, in which 2.7MW of LHCD power is coupled during 8s in an H-mode plasma with high frequency ($>100\text{Hz}$), small amplitude ELMs. The gas flow near the launcher was $5 \times 10^{21}\text{el/s}$ and the average power reflection coefficient was 4-6%.

From the LHCD point of view, the parameter to take into account in this low toroidal magnetic field scenario is the reduced accessibility of the LH wave. The accessibility condition, $n_{//}^{\text{acc}}$, is given by [13, 14]:

$$n_{//}^{\text{acc}} = \frac{\omega_{\text{pe}}}{\omega_{\text{ce}}} + \sqrt{1 + \left(\frac{\omega_{\text{pe}}}{\omega_{\text{ce}}}\right)^2 - \left(\frac{\omega_{\text{pi}}}{\omega}\right)^2}$$

where ω is the wave frequency, ω_{pe} the local electron plasma frequency, ω_{pi} the local ion plasma frequency and ω_{ce} the local electron cyclotron frequency, respectively. The LH wave accessibility therefore depends on the local electron density and magnetic field. Waves with $n_{//} > n_{//}^{\text{acc}}$ are accessible to the plasma interior, while waves with $n_{//} < n_{//}^{\text{acc}}$ will be reflected at that layer. For the scenario shown in Fig. 5, the minimum $n_{//}$ accessible is as high as $n_{//}^{\text{acc}} \sim 3.0$ at $R = 3.7\text{m}$ ($r/a = 0.8$). Therefore, the highest $n_{//}$ -spectrum was also used in the experiment ($n_{//} = 2.3$) and compared to the standard $n_{//}$ -spectrum peaked at 1.84, which corresponds to the highest power directivity. In plasmas suffering from poor LH wave accessibility, one may find increased impurity production, as reported in JT-60U [15]. However, in this JET experiment no difference in impurity production between $n_{//} = 1.84$ and $n_{//} = 2.3$ could be observed. The difference in coupling between the two phasings was small, although $n_{//} = 1.8$ had a slightly lower reflection coefficient than $n_{//} = 2.3$. A

comparison of two consecutive discharges with different $n_{||}$ -spectrum show that the average RC during the L-mode phase (4.0-4.5s) was 4% for $n_{||} = 1.84$, increasing to 6% for $n_{||} = 2.3$. During the H-mode phase (5.5-7.0s), the average RC was 7% for $n_{||} = 1.84$, increasing to 8% for $n_{||} = 2.3$. This is in agreement with SWAN code calculations, which predict a minimum in reflection coefficient for 0° phasing between adjacent multijunctions [16]. The 0° phasing ($n_{||}=1.84$) gives a continuous phase difference between the narrow waveguides at the grill mouth of 90° , which corresponds to the optimum feeding of the launcher and the highest power directivity.

4. EFFECTS OF GAS PUFFING ON PLASMA PERFORMANCE AND LHCD EFFICIENCY

4.1. EFFECT ON PLASMA PERFORMANCE

When using high levels of gas injection, a degradation in the H-mode confinement may be encountered due to reduced pedestal electron temperature and increased collisionality [17]. The series of discharges in the Hybrid scenario experiment allowed to study the evolution of the normalised plasma pressure, β_N , and the normalised H-mode confinement, $H98(y,2)$ [18]. In this experiment, β_N was controlled in real-time by adjusting the NBI power so as to maintain $\beta_N = 2.0$ between 6s and 7.5s, and then $\beta_N = 2.5$ between 8s and 12s. A typical NBI power waveform is shown in figure 5. Since the main aim was to reach large distance LH coupling conditions, the distance of the LCFS to the poloidal limiter and the GIM6 flow were increased from discharge to discharge. The LCFS-limiter distance was varied between 4cm and 12cm, while the GIM6 flow was varied between 2×10^{21} el/s and 8×10^{21} el/s. An increase in the base-line level of the $H\alpha$ -signal from discharge to discharge could be observed. This increase can be attributed to the increasing level of gas puffing. In order to maintain the requested value of β_N , the NBI power which was real-time controlled had to increase from discharge to discharge. In fact, the increase in applied NBI power could therefore indicate a degradation in confinement due to the increased level of gas puffing. Figure 6 shows $H98(y,2)$ at two different times, plotted versus the average electron density normalised to the Greenwald density limit, n_e/n_G [19].

As seen in figure 6, the discharges with $n_{||}=2.3$, as well as the discharge without LH during the main heating phase, differ slightly from the rest of the data points. This could possibly be attributed to the different MHD activity, caused by different LH driven current profiles. Experimentally, a clear difference in the MHD activity was observed between the discharges with $n_{||} = 1.84$ and 2.3. In the pulse with $n_{||} = 1.84$, a continuous $m = 3$, $n = 2$ mode remained throughout the high performance phase, while no MHD events associated with the sawtooth or fishbone activity were observed, indicating the absence of the $q = 1$ surface in the plasma. The lower H-mode confinement may therefore possibly be explained by the presence of the $m/n = 3/2$ mode, causing a degradation in confinement [20]. In contrast, in the pulse with $n_{||} = 2.3$ or in the pulse without LHCD in the main heating phase, only MHD activity associated with sawteeth and fishbones were detected, suggesting the presence of a $q = 1$ surface. Preliminary simulations with the DELPHINE code [21] coupled

with CRONOS [22] for the discharge in figure 5 indicate that the LH power deposition during the high performance phase is localised around $r/a = 0.6-0.8$, both for $n_{//} = 1.84$ and 2.3 , but for $n_{//} = 2.3$ there is an additional peak in LH power absorption close to the plasma centre ($r/a < 0.2$). This is not inconsistent with the appearance of sawteeth for $n_{//} = 2.3$.

In addition to the different MHD behaviour, it is also interesting to note that the divertor $H\alpha$ -signal for the discharges with LHCD at $n_{//} = 2.3$ were lower than in the discharges at $n_{//} = 1.84$, for the same amount of GIM6 flow and same LCFS-limiter distance. When plotting $H98(y,2)$ versus the base-line level of the divertor $H\alpha$ -signal, a better correlation than with n_e/n_G is observed (figure 7). This could probably be explained by the fact that the wave propagation at the peripheral plasma is different due to different LH wave accessibility, as described in Section 3.2. The waves with $n_{//} = 1.84$ suffer from poor accessibility during the main heating phase in this scenario, which can lead to multiple reflections and higher LH power loss at the periphery.

The results in figures 6 and 7 indicate a degradation in performance at increasing $H\alpha$ level, mainly due to gas puffing from GIM6. However, these results do not allow to distinguish between the effect of gas puffing from GIM6 (outer mid plane) or from other gas flow locations (e.g. from the divertor). The experiment described in Section 3.1 allows to address this issue, since different combinations of gas injection locations were used. The scenario was the advanced tokamak scenario, but since the experiment was performed early during the development campaign, internal transport barriers were not obtained. The H-mode was characterised by type I ELMs, for which the ELM frequency increased with increasing amount of gas puffing. Figure 8 shows $H98(y,2)$ versus the electron density normalised to the Greenwald density limit, n_e/n_G , for discharges characterised by an upper triangularity $\delta_{up} = 0.38 - 0.41$ and $q_{05} = 5.5 - 6.8$. The various GIM6 levels can be distinguished. The points corresponding to zero flow from GIM6 have gas injection from the divertor region. From figure 8, there does not seem to be any difference in confinement, whether GIM6 is used or not. However, further experiments are necessary in order to verify the experimental result of figure 8 in higher confinement scenarios, with $H98(y,2) = 1$ or above.

4.2 EFFECT ON LH CURRENT DRIVE EFFICIENCY

When using near gas puffing to improve the LH coupling, possible deleterious effects due to parasitic absorption of the LHCD power in front of the launcher at excessive local electron density could be an important issue. Such effects could translate into increased heat flux carried by the electrons accelerated near the grill mouth and possibly a decrease in the LH current drive (CD) efficiency. The figure of merit for the LH current drive efficiency (η) is given by: $\eta = RI_{LH} n_e / P_{LH}$ (in units of $10^{20} \text{Am}^{-2}/\text{W}$), where R is the plasma major radius, n_e the line average electron density, I_{LH} the LH driven non-inductive current and P_{LH} the LHCD power. An experiment has recently been carried out in JET in order to investigate this issue.

For simplicity, it was carried out in L- mode plasmas with 2.8MW LHCD, with the addition of 1MW ICRH power in order to increase the plasma electron temperature thereby improving

the LHCD efficiency. Real-time control on the boundary flux was used, in order to keep the loop voltage constant and leave the plasma current floating. The amount of gas injected near the LH launcher (from GIM6) and the distance from the LCFS to the poloidal limiter (ROG) were varied from discharge to discharge, while parameters such as electron density, electron temperature, total gas injection and LHCD power, were kept the same. In such a way, a variation in the LH current drive efficiency was detected by a variation in the resulting plasma current.

The plasma parameters for the two extreme cases in the scan are shown in figure 9. The highest plasma current was indeed obtained for the case with small LCFS-limiter distance without gas injection near the launcher (#69581), while the lowest plasma current was obtained in the other extreme case with 10cm distance between the LCFS and the poloidal limiter and GIM6 flow of 4×10^{21} e/s (#69582). The divertor H α -signal also differs for the two discharges. A higher amplitude and larger fluctuation level is seen from 8s onwards in #69582. Figure 10 shows the fluctuation level at the plasma periphery, measured by O-mode reflectometry, with the channel having its cut-off density at $1.1 \times 10^{19} \text{ m}^{-3}$. One can note that the lowest fluctuation level is clearly obtained for #69581, i.e. the discharge with small LCFS-limiter distance without GIM6, while the highest fluctuation levels are obtained for #69582 and #69576, which are the two discharges with the largest LCFS-limiter distance (10cm) and gas injection from GIM6 with 4×10^{21} e/s and 2×10^{21} e/s, respectively. This result is possibly a first indication that LH wave scattering in the SOL region is enhanced in cases with a wide SOL combined with local gas puffing. LH wave scattering may modify the LH wave propagation, as described in [23].

Simulations with the DELPHINE code coupled with CRONOS indicate that the LH driven current was only 0.4MA in this experiment, i.e. approximately 30% of the total current, while the bootstrap current was 0.1MA. However, the density could not be maintained constant during the pulse (due to the gas puffing), which caused the current profiles (ohmic as well as LH driven current profile) to evolve during the pulse. Since stationary conditions were obtained in this experiment, it is difficult to accurately quantify the degradation in current drive efficiency, as caused by large ROG and gas puffing. The simplest estimates would give the following: The difference in plasma current between the two extreme discharges, #69581 and #69582, is roughly 60kA, which can be considered as the difference in LH driven current, i.e. $\Delta I_{\text{LH}} \sim 60\text{kA}$. CRONOS code modelling gives an absolute value of the LH driven current of $I_{\text{LH}} \sim 400\text{kA}$ in this specific scenario. The drop in current drive efficiency would therefore correspond to $\Delta I_{\text{LH}}/I_{\text{LH}} \sim 15\%$. This effect is indeed small in comparison to the loss of coupled power that would be the result if local gas puffing was not used for improving the LH coupling at large distance (as illustrated in figure 3).

5. MODELLING OF GAS PUFF

The density increase in front of the launcher has been studied numerically with the 2-dimensional code EDGE-2D [24, 25]. For this purpose, the code has been extended to account for a SOL width of up to 10cm. In this model, the effect of LHCD power is taken into account by assuming that a

certain fraction of the power is absorbed within the narrow band in front of the launcher. Consequently, the plasma in this narrow band heats up locally and this then contributes to the ionisation of the gas. This way the code takes into account the direct effect of LHCD power on the ionisation. The poloidal limiters have been modelled as spatially localised sinks, where the recombination is artificially enhanced [26]. This makes it possible to distinguish the private space of the LH launcher. The private space between the limiters is important for the coupling as the density in this region may decrease to values below the cut-off density. This model then allows studying various gas puffing options, e.g. outer mid plane (as is used for the LH coupling improvement in JET) or top gas injection (the location of which is foreseen to provide the main gas injection in ITER). However, since the model is 2D the gas puff location is always magnetically connected to the LH launcher, and it is impossible to distinguish between connected or not connected cases.

The results of the simulations with different gas puff locations, with and without heating, are shown in figure 11. The figure shows the effect of gas injection at a level of 1×10^{22} e/s, without any direct SOL heating by LH waves (dashed curves with squares and circles) and with heating 50 kW (full curves with squares and circles). Gas injection at the outer mid-plane (squares) is clearly more favourable for increasing the density at the outer mid-plane than gas injection from the top (circles). However, the density at the wall (LH launcher position) increases to $1 \times 10^{18} \text{ m}^{-3}$ with both gas puffing locations and with SOL heating, although the outer mid plane gas puffing is the more favourable. This modelling indicates that gas puffing from the top of the torus, as is foreseen in ITER, could also be suitable for improving the LH coupling in ITER. In that case, a dedicated gas injection pipe close to the LH launcher would no longer be necessary. Further experiments to study this experimentally have therefore been proposed in JET.

SUMMARY AND CONCLUSIONS

Good coupling of LHCD power in H-mode plasmas with high frequency type I ELMs, at high triangularity and ITER-relevant plasma-launcher distance, has been demonstrated in JET. 2.7MW of LHCD power has been maintained during 8s with a distance between the LCFS and the launcher of 14cm. Higher LHCD power has been coupled for shorter periods (3.1MW / 3s) at 15cm distance between the LCFS and the launcher. At large LCFS-launcher distance, gas injection in the scrape-off layer magnetically connected to the LH launcher is an essential tool for ensuring good coupling. Reciprocating Langmuir probe measurements show that the ion saturation current profile flattens in the far SOL, resulting in an increase in electron density in front of the LH launcher.

The modelling effort using the 2D code EDGE-2D confirms the increased density when using both gas puffing and LHCD power. Simulations varying the gas puffing location suggest that the outer mid plane is obviously the most favourable, but that gas puffing from the top of the torus (as foreseen for the main gas injection in ITER) could also be efficient. However, a 3D analysis would be needed to fully model the SOL during gas puffing. The possibility to use gas injection from the top of the torus to improve LH coupling will be investigated in future experiment in JET.

The effect of gas injection, as needed for LH coupling, on the plasma performance was investigated during the LH coupling experiments. However, the experiments were performed in scenarios with modest normalised H-mode confinement, $H_{98}(y,2)$, that are not representative of the highest performance scenarios in JET. From the available data, no difference between gas injection near the LH launcher or from the divertor can be found. In the scenarios studied, $H_{98}(y,2)$ decreases as the density normalised to the Greenwald density limit increases, whether gas is puffed near the launcher or far way from it. A more systematic study in higher confinement regimes are planned in order to verify that the gas injection near the LH launcher (outer mid plane) does not have a greater influence on confinement degradation than gas injection from the divertor.

The effect on the LH current drive efficiency during near gas puffing has also been investigated. The results obtained seem to indicate a small decrease in LH driven current (by $\sim 15\%$) at large LCFS-launcher distance assisted by near gas injection, compared to the case with small distance between the LCFS and the launcher, where near gas injection is not needed. It should be noted that such a small decrease in current drive efficiency is small in comparison to what would be the loss of coupled LHCD power if not assisted by local gas injection at large distance.

In conclusion, the experiments presented here do not indicate any drastic negative effects neither in confinement, nor in LH current drive efficiency, linked to the near gas injection used for improving the LH coupling at ITER-relevant plasma-launcher distances.

ACKNOWLEDGMENTS

The authors acknowledge the support of the UKAEA JET Operator of the JET EFDA Facility. The support of the UKAEA Heating and Fuelling Department, and in particular of the LHCD Team, is gratefully acknowledged. This work, supported by the European Communities under the contract of Association between EURATOM and CEA, was carried out within the framework of the European Fusion Development Agreement. The views and opinions expressed herein do not necessarily reflect those of the European Commission. One of the authors (V. Petrzilka) was supported in part by the Czech Science Foundation Project GACR 202/07/0044 and by MSMT CR Grant# LA08048”.

REFERENCES

1. P.T. Bonoli et al., Proceedings of 15th Topical Conf. on Radio Frequency Power in Plasmas, Moran, Wyoming, USA (2003). AIP Conference Proceedings 694, (Melville, New York, 2003) 24-37.
2. C. Challis, Plasma Phys. Control. Fusion 46 (2004) B23-B40.
3. J. Mailloux et al., Phys. Plasmas 9 (2002) 2156.
4. F. Leuterer et al., Plasma Phys. Control. Fusion 33 (1991) 169.
5. M. Lennholm et al., Proc. 16th Symposium on Fusion Engineering, Urbana-Champaign, Illinois (1995), vol. 1, p. 754.
6. Ph. Schild et al., Proc. 17th Symposium on Fusion Engineering, San Diego, CA (1997),

vol. 1, p. 421.

7. V. Pericoli Ridolfini et al., *Plasma Phys. Control. Fusion* 46 (2004) 349.
8. A. Ekedahl et al., *Nucl. Fusion* 45 (2005) 351.
9. K. Rantamäki et al., *Proceedings of 17th Topical Conf. on Radio Frequency Power in Plasmas*, Clearwater, Florida, USA (2007). *AIP Conference Proceedings* 933, (Melville, New York, 2007) 261-264.
10. M.-L. Mayoral et al., *Proceedings of 17th Topical Conf. on Radio Frequency Power in Plasmas*, Clearwater, Florida, USA (2007). *AIP Conference Proceedings* 933, (Melville, New York, 2007) 55-58.
11. S.K. Erents et al, *Plasma Phys. Control. Fusion* 42 (2000) 905.
12. E. Joffrin et al., *Nucl. Fusion* 45 (2005) 626.
13. T.H. Stix, *The Theory of Plasma Waves*, McGraw-Hill, New York, USA (1962).
14. V.E. Golant, *Sov. Phys. – Tech. Phys.* 16 (1972) 1980.
15. Y. Ikeda et al., *Nucl. Fusion* 34 (1994) 871.
16. A Ekedahl et al., *Proceedings of 14th Topical Conf. on Radio Frequency Power in Plasmas*, Oxnard, CA, USA (2001). *AIP Conference Proceedings* 595, (Melville, New York, 2001) 249-252.
17. G. Saibene et al., *Nucl. Fusion* 39 (1999) 1133.
18. ITER Physics Basis Editors, *Nucl. Fusion* 39 (1999) 2175.
19. M. Greenwald et al., *Nucl. Fusion* 28 (1988) 2199.
20. R. Buttery et al., *Nucl. Fusion* 43 (2003) 69.
21. F. Imbeaux and Y. Peysson, *Plasma Phys. Control. Fusion* 47 (2005) 2041.
22. V. Basiuk et al., *Nucl. Fusion* 43 (2003) 822.
23. R. Cesario et al., *Nucl. Fusion* 46 (2006) 462.
24. R. Simonini, G. Corrigan, G. Radford, J. Spence, A. Taroni, *Contrib. Plasma Phys.* 34 (1994) 2/3 368-373.
25. V. Petrzilka et al., “SOL Ionization by the Lower Hybrid Wave During Gas Puffing”, *Proceedings of 33rd EPS Conf. on Plasma Physics*, Rome, Italy (2006). Paper P-1.06.
26. V. Petrzilka et al., “Near LH Grill Density Variations as a Function of Gas Puff and LH Power”, *Proceedings of 34th EPS Conf. on Plasma Physics*, Warsaw, Poland (2007). Paper P4.100.

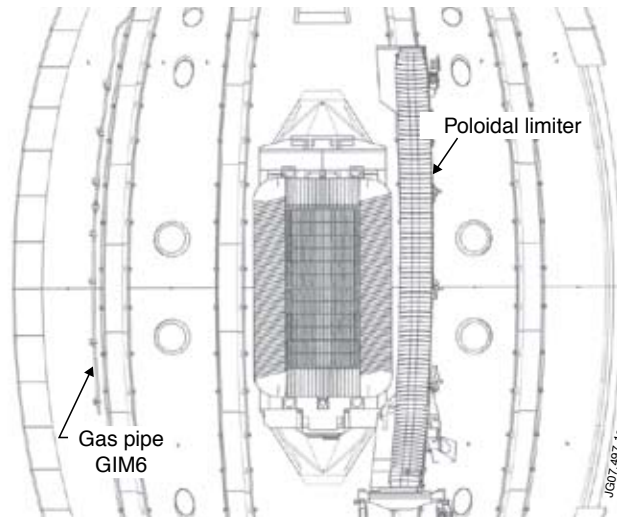


Figure 1: Front view of the Lower Hybrid launcher in JET. The gas injection pipe (GIM6) is seen to the left of the launcher and a poloidal limiter to the right. Immediately to the right of the poloidal limiter is an ICRH antenna (not shown in the figure).

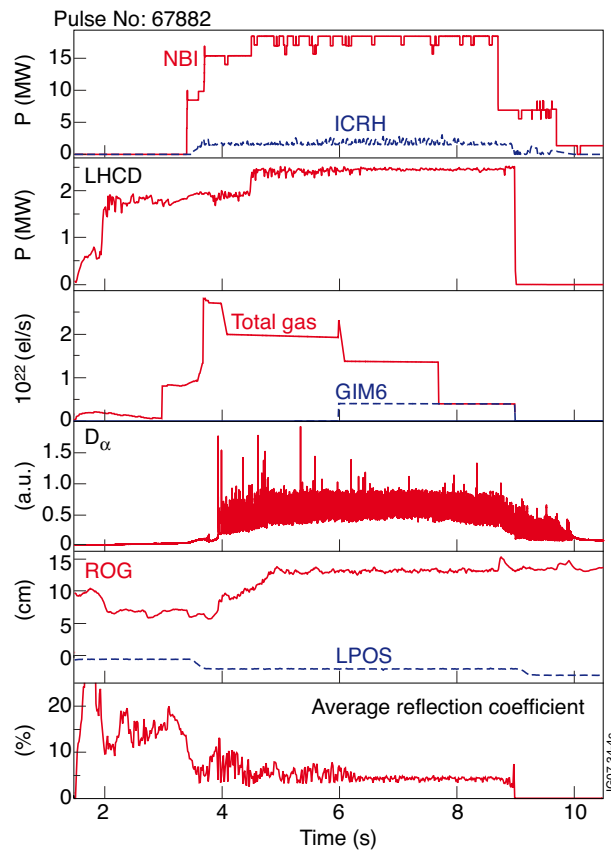


Figure 2: Illustration of long distance LH coupling, in a case with large gas flow from the divertor. Good coupling is obtained even without GIM6 injection (4-6s). Shown are as function of time: NBI and ICRH powers, coupled LHCD power, total gas flow and near gas flow from GIM6, the D_{α} signal showing the ELM activity, the positions of the LCFS relative to the poloidal limiter (ROG) and the LH launcher relative to the poloidal limiter (LPOS), and the average reflection coefficient on the LH launcher.

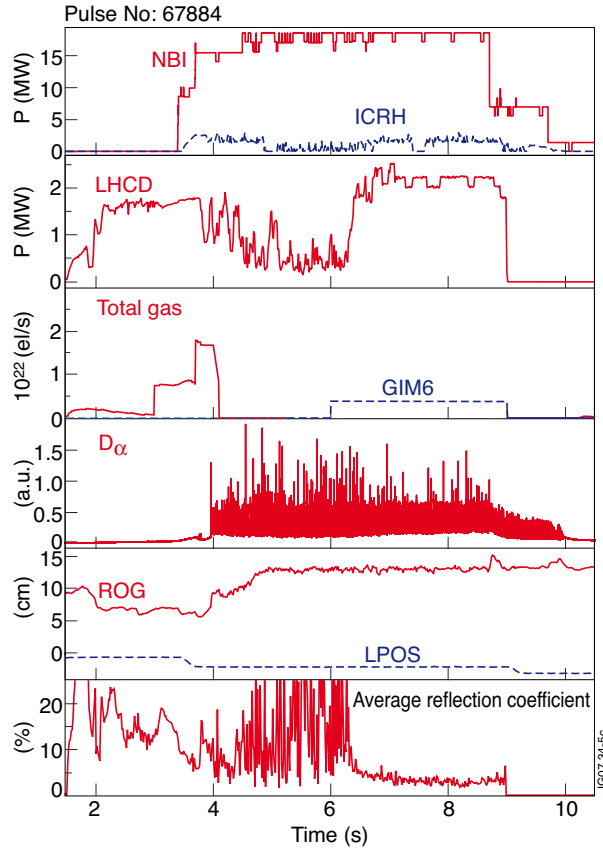


Figure 3: Illustration of long distance LH coupling experiment, in a case with only GIM6 injection, or no gas injection, during the H-mode phase. The coupling is degraded over the whole launcher when no gas is injected (4-6s).

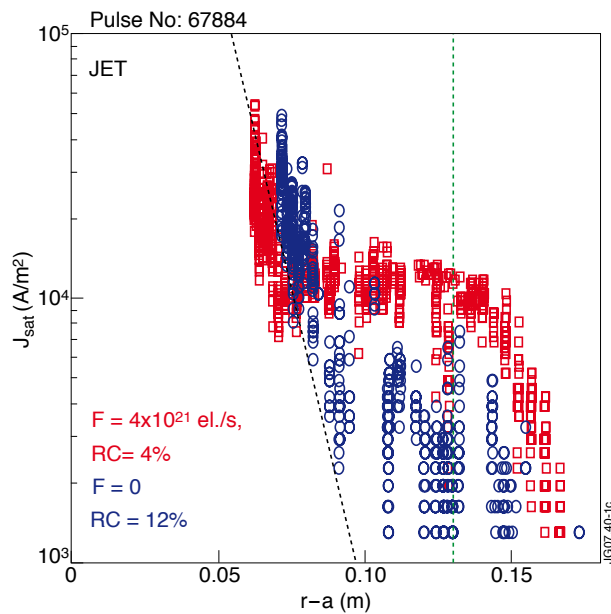


Figure 4: Ion saturation current measured by the reciprocating probe in #67884 as a function of the distance from the separatrix mapped to the mid-plane. With GIM6 and PLH = 2MW, $t = 7$ s (squares), without GIM6, $t = 5$ s (circles).

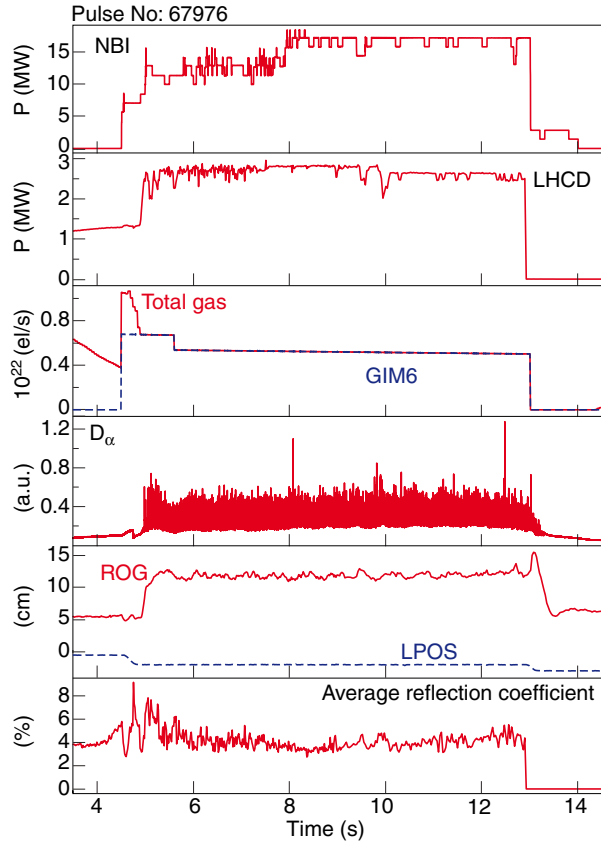


Figure 5: Illustration of LH coupling in hybrid scenario at $B_T = 1.7T$. Shown are as function of time: NBI and ICRH powers, coupled LHCD power, total gas flow and the near gas flow from GIM6, the D_α signal showing the ELM activity, the positions of the LCFS relative to the poloidal limiter (ROG) and the LH launcher relative to the poloidal limiter (LPOS), and the average reflection coefficient on the LH launcher.

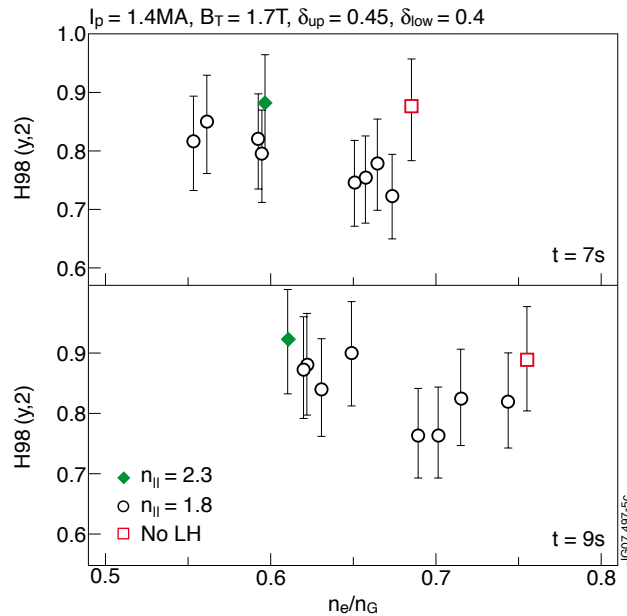


Figure 6: $H_{98}(y,2)$ versus n_e/n_G for the discharges in the Hybrid scenario experiment at $B_T = 1.7T$ (figure 4). The pulse indicated as “no LH” has only LH in the pre-heat phase up to 5s (with $n_{||}=1.8$).

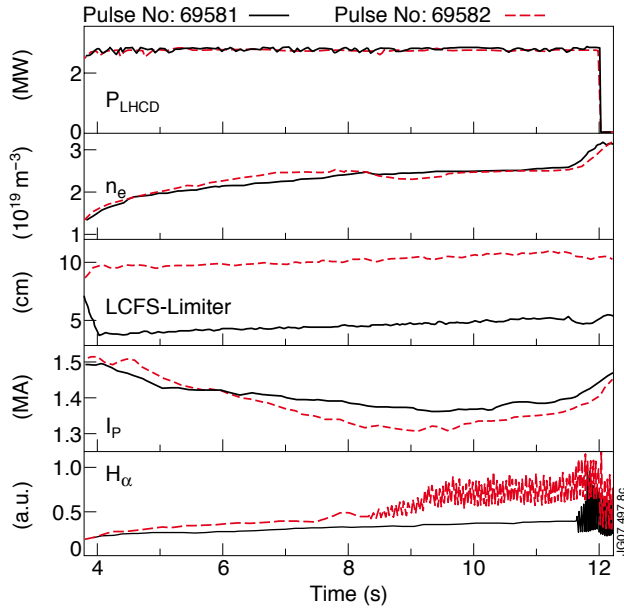


Figure 9: Evolution of plasma parameters for two discharges with real-time control on plasma boundary flux. Shown are: Coupled LHCD power, line average electron density, LCFS-limiter distance (ROG), plasma current and divertor $H\alpha$ -signal. #69581 has gas injection from the divertor, while #69582 has gas injection near the LH launcher.

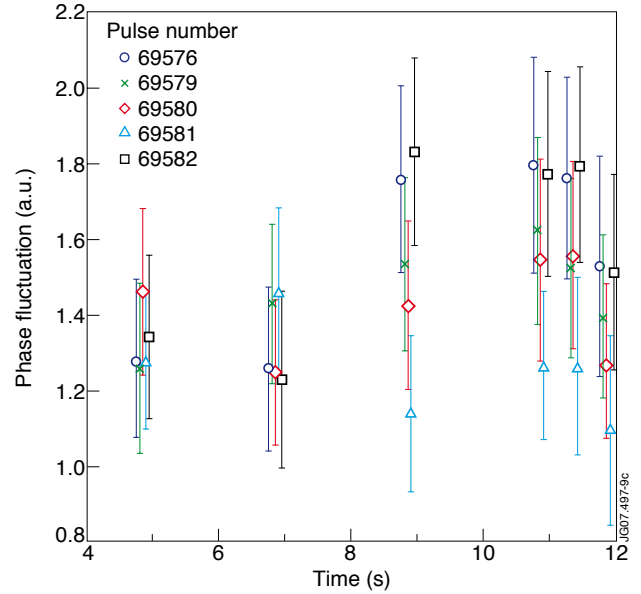


Figure 10: Fluctuation level measured by O-mode reflectometry at the plasma periphery (cut-off density = $1.1 \times 10^{19} \text{ m}^{-3}$).

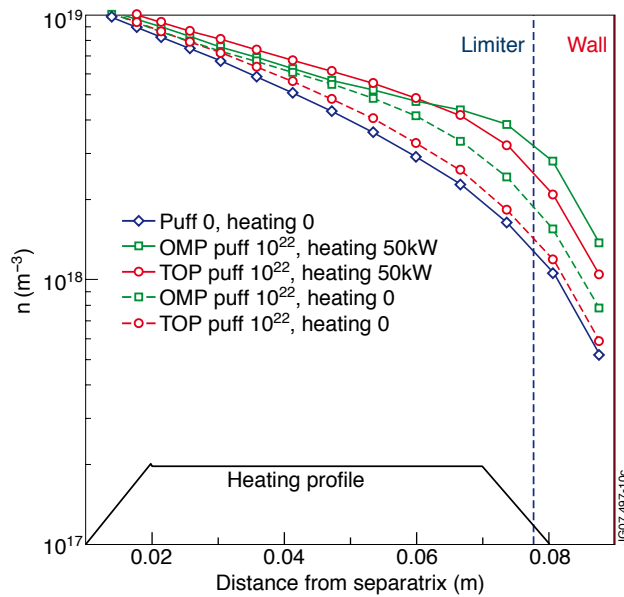


Figure 11: EDGE-2D modelling of the far scrape-off layer during gas puffing in JET for the configuration of pulse #66972: Electron density profile at the outer mid plane with gas puffing at $1 \times 10^{22} \text{ el/s}$ from the outer mid-plane (squares) and from the top of the torus (circles). Dashed curves are with zero heating, full curves (squares and circles) are with heating 50kW. The reference profile without gas puffing and with zero heating is indicated with diamonds.

